

Geometry-Aware Metric Learning for Cross-Lingual Few-Shot Sign Language Recognition on Static Hand Keypoints

Chayanin Chamachot
Department of Computer Engineering
Faculty of Engineering, Chulalongkorn University

Kanokphan Lertniphonphan
Department of Computer Engineering
Faculty of Engineering, Chulalongkorn University

Abstract

Sign-language recognition (SLR) systems typically require large labelled corpora for each language, yet the majority of the world’s 300+ sign languages lack sufficient annotated data. Cross-lingual few-shot transfer—pretraining on a data-rich source language and adapting with only a handful of target-language examples—offers a scalable alternative, but conventional coordinate-based keypoint representations are susceptible to domain shift arising from differences in camera viewpoint, hand scale, and recording conditions. This shift is particularly detrimental in the few-shot regime, where class prototypes estimated from only K examples are highly sensitive to extrinsic variance. We propose a geometry-aware metric-learning framework centred on a compact 20-dimensional inter-joint angle descriptor derived from MediaPipe static hand keypoints. These angles are provably invariant to $SO(3)$ rotation, translation, and isotropic scaling, thereby eliminating the dominant sources of cross-dataset shift and yielding tighter, more stable class prototypes. Evaluated on four fingerspelling alphabets spanning typologically diverse sign languages—ASL, LIBRAS, Arabic SL, and Thai—the proposed angle features improve over normalised-coordinate baselines by up to 25 percentage points within-domain and enable frozen cross-lingual transfer that frequently exceeds within-domain accuracy, all using a lightweight MLP encoder (~ 105 k parameters). These findings demonstrate that formally invariant hand-geometry descriptors provide a portable and effective foundation for cross-lingual few-shot SLR in low-resource settings.¹

¹Code and data splits are available at https://github.com/fjkrch/sign_metric_learning.

1. Introduction

Sign language is the primary mode of communication for over 70 million Deaf individuals worldwide [28], yet recognition technology currently serves only a small fraction of the 300+ documented sign languages [12]. Building an SLR system for an under-resourced language typically requires thousands of labelled examples per class—a requirement that is prohibitively expensive for most communities. This data bottleneck motivates *cross-lingual few-shot transfer*: pretraining a model on a data-rich source language and adapting it to a new target language using only a handful of labelled examples.

Challenge: domain shift in keypoint representations.

State-of-the-art continuous SLR systems fuse RGB, optical flow, and body/hand keypoints [5, 17], but they depend on large video corpora and learn language-specific patterns. Existing isolated SLR benchmarks evaluate single-language, closed-set classification [2, 19, 21], leaving it unclear whether learned representations generalise across languages. Although cross-lingual transfer is well studied in NLP [9] and speech [18], it remains largely unexplored for sign languages; Tavella *et al.* [26] apply few-shot learning to signs but only within a single language. A key obstacle is that normalised (x, y, z) keypoint coordinates remain sensitive to camera viewpoint and hand scale, inducing domain shift across datasets collected under different conditions. In the few-shot regime this problem is amplified: each Prototypical Network centroid is estimated as a sample mean over only K examples, so extrinsic variance in the input directly inflates prototype estimates and destabilises classification.

Our approach. We propose a *transferable geometric inductive bias*: a set of 20 inter-joint angles computed from MediaPipe [29] static hand keypoints, provably invariant to

rotation, translation, and isotropic scaling (Sec. 3.2). Figure 1 illustrates the full pipeline: a hand image is processed by MediaPipe into 21 keypoints, converted to one of three representations (`raw`, `angle`, or `raw_angle`), and encoded into a 128-dimensional embedding for Prototypical Network classification. Using a lightweight MLP encoder (~ 105 k parameters), we evaluate on four typologically diverse fingerspelling alphabets—**ASL** (29 classes), **LIBRAS** (21), **Arabic SL** (31), and **Thai** (42)—under a deterministic 5-way K -shot protocol. Because the angle embedding is intrinsically invariant to rigid transforms, it requires no spatial normalisation across camera setups, is more privacy-preserving than RGB pipelines (only keypoints and angles are stored), and can serve as a plug-in pose branch in multi-modal architectures.

Contributions.

1. **Cross-lingual few-shot benchmark.** We establish a deterministic 5-way K -shot evaluation protocol spanning four typologically diverse fingerspelling alphabets. Angle features frequently match or exceed within-domain baselines under cross-lingual transfer (Tabs. 3, 4 and 6).
2. **Geometry-invariant representation.** We derive a 20-dimensional inter-joint angle feature that is provably invariant to rotation, translation, and isotropic scaling (Eq. (7)). Removing normalisation degrades `raw` coordinates by ~ 5 pp, while angle features remain unchanged ($|\Delta| \leq 0.3$ pp; Tabs. 7 and 8).
3. **Systematic baselines.** We benchmark few-shot accuracy against input-space, episode-linear, full-data, and multi-seed baselines (Tab. 9), quantifying the cost of learning from only K examples.

Scope. This work evaluates isolated, static fingerspelling—not continuous SLR—using keypoints only, and is complementary to video-based approaches.

2. Related Work

We organise prior work into four areas: skeleton-based representations, single-language SLR, few-shot learning for sign recognition, and cross-lingual or zero-shot transfer.

Skeleton and keypoint-based representations. MediaPipe Hands [29] provides real-time 21-keypoint hand tracking, enabling lightweight SLR pipelines that typically flatten (x, y, z) coordinates into a 63-dimensional vector [10, 23]. Jiang *et al.* [15] demonstrate that skeleton features generalise better than appearance-based features across recording conditions; however, they do not evaluate cross-lingual transfer. Angle-based descriptors have a long history in action recognition [7, 22] and glove-based gesture systems [8], yet existing MediaPipe SLR pipelines have not exploited them.

Our 20-dimensional angle representation (Sec. 3.2) achieves exact $SO(3)$ invariance under similarity transforms (Eq. (7)), enabling stable cross-dataset transfer without ad-hoc normalisation.

Single-language sign language recognition. CNN-based methods achieve over 99% accuracy on the ASL Alphabet benchmark [19]; hand-crafted skeleton features reach 97% on LIBRAS [21] and Arabic SL [2]; graph convolutional networks further advance continuous SLR [17]. All of these approaches are *single-language*: they require large per-class training sets and do not address cross-lingual generalisation.

Few-shot learning for sign recognition. Prototypical Networks [24] learn a metric embedding space in which classification reduces to nearest-centroid matching. Chen *et al.* [6] demonstrate that a well-tuned ProtoNet often matches more complex meta-learning alternatives such as MAML [13], Matching Networks [27], and Relation Networks [25]. Tavella *et al.* [26] apply few-shot learning to sign language but evaluate only within a single language, leaving the cross-lingual setting unexplored.

Cross-lingual and zero-shot SLR. Boháček [4] explores pose-based few-shot SLR on ASLLVD-Skeleton but is limited to a single language. Bilge *et al.* [3] investigate zero- and few-shot SLR across ASL, DGS, and TID but rely on fully supervised target-language training. Our work differs from both in three respects: (i) we adopt a deterministic N -way K -shot episodic protocol, (ii) we introduce formally invariant geometric features that remove extrinsic variance at the representation level, and (iii) we evaluate cross-lingual transfer across four typologically diverse languages.

3. Method

Our framework comprises four stages: (1) extraction of 21 hand keypoints via MediaPipe, (2) conversion to an $SO(3)$ -invariant angle descriptor (Sec. 3.2), (3) encoding into a 128-dimensional embedding (Sec. 3.3), and (4) classification by nearest-prototype matching (Sec. 3.4). Figure 1 illustrates the complete pipeline.

3.1. Keypoints and Raw-Coordinate Preprocessing

Given a hand image, we extract 21 three-dimensional landmarks $\{\mathbf{p}_i\}_{i=0}^{20}$ using MediaPipe Hands [29], where each landmark $\mathbf{p}_i = (x_i, y_i, z_i) \in \mathbb{R}^3$ represents the spatial position of a hand joint. Keypoint \mathbf{p}_0 corresponds to the wrist and serves as the root of the hand skeleton. The remaining 20 keypoints are arranged in five four-joint kinematic chains—Thumb (indices 1–4), Index (5–8), Middle (9–12), Ring (13–16), and Pinky (17–20)—as depicted in Fig. 2.

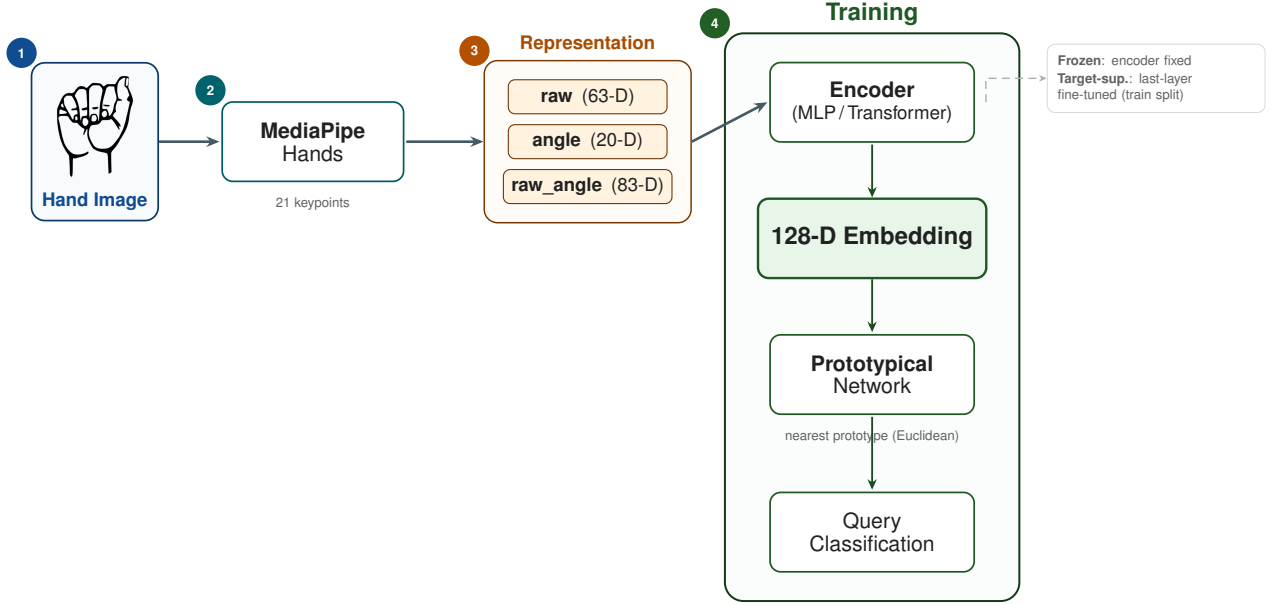


Figure 1. Pipeline overview. A hand image is processed by MediaPipe Hands into 21 keypoints (63-D when flattened), converted to one of three representations—*raw* (63-D), *angle* (20-D), or *raw_angle* (83-D)—and encoded into a 128-D embedding for Prototypical Network classification. In the cross-lingual setting, the encoder is either *frozen* or undergoes *target-supervised adaptation* (last-layer fine-tuning on the target train split).

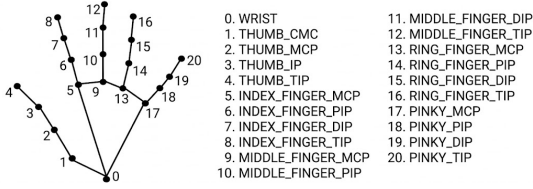


Figure 2. MediaPipe Hands keypoint topology ($i \in \{0, \dots, 20\}$). Keypoint 0 is the wrist (root); each finger forms a four-joint kinematic chain following the official ordering [29]: Thumb (1–4), Index (5–8), Middle (9–12), Ring (13–16), Pinky (17–20).

The **raw** coordinate representation is obtained through two normalisation steps:

1. **Translation invariance (wrist-centring)**. The wrist position is subtracted from all keypoints to remove global translation:

$$\hat{\mathbf{p}}_i = \mathbf{p}_i - \mathbf{p}_0, \quad i \in \{0, \dots, 20\}. \quad (1)$$

2. **Scale invariance**. All centred keypoints are divided by the maximum pairwise distance, removing dependence on hand scale and camera distance:

$$\tilde{\mathbf{p}}_i = \frac{\hat{\mathbf{p}}_i}{\max_{j,k \in \{0, \dots, 20\}} \|\hat{\mathbf{p}}_j - \hat{\mathbf{p}}_k\|}, \quad i \in \{0, \dots, 20\}. \quad (2)$$

The resulting **raw** representation is obtained by row-major flattening of the normalised keypoints:

$$\mathbf{x}_{\text{raw}} = \text{vec}(\tilde{\mathbf{p}}_0, \tilde{\mathbf{p}}_1, \dots, \tilde{\mathbf{p}}_{20}) \in \mathbb{R}^{63}, \quad (3)$$

where $\text{vec}(\cdot)$ denotes concatenation of all coordinate components and $63 = 21 \times 3$. Importantly, the angle representation introduced next is computed from the *original* (unnormalised) keypoints $\{\mathbf{p}_i\}$ and does not depend on the normalisation steps above.

3.2. Geometry-Aware Angle Representation

The 21-keypoint hand skeleton forms a kinematic tree rooted at the wrist (\mathbf{p}_0 ; see Fig. 2). Each non-wrist keypoint has a unique parent in this tree, producing 20 anatomical triplets (a_k, j_k, c_k) for $k \in \{1, \dots, 20\}$, where a_k , j_k , and c_k denote the *parent*, *joint* (pivot), and *child* keypoint indices, respectively. Each triplet connects consecutive links along a finger chain. As a concrete example, $(a_k, j_k, c_k) = (5, 6, 7)$ measures flexion at the proximal interphalangeal (PIP) joint of the index finger, with keypoint 5 (MCP) as parent, 6 (PIP) as pivot, and 7 (DIP) as child.

For each triplet, we define displacement vectors from the pivot to its parent and child:

$$\mathbf{u}_k = \mathbf{p}_{a_k} - \mathbf{p}_{j_k}, \quad \mathbf{v}_k = \mathbf{p}_{c_k} - \mathbf{p}_{j_k}, \quad (4)$$

The inter-joint angle is then computed via the normalised dot product:

$$\theta_k = \arccos\left(\frac{\mathbf{u}_k \cdot \mathbf{v}_k}{\|\mathbf{u}_k\| \|\mathbf{v}_k\|}\right), \quad k \in \{1, \dots, 20\}, \quad (5)$$

where $\|\cdot\|$ denotes the Euclidean norm and \cdot the standard inner product in \mathbb{R}^3 . Since there are exactly 20 non-wrist joints

in the hand skeleton, this procedure yields the **angle** representation $\mathbf{x}_{\text{angle}} \in \mathbb{R}^{20}$. To combine positional and angular cues, we additionally form the **raw_angle** concatenation:

$$\mathbf{x}_{\text{raw_angle}} = [\mathbf{x}_{\text{raw}}; \mathbf{x}_{\text{angle}}] \in \mathbb{R}^{83}, \quad (6)$$

where $[\cdot; \cdot]$ denotes vector concatenation and $83 = 63 + 20$.

Invariance property. A central advantage of the angle representation is its provable invariance to similarity transforms. Let $T: \mathbf{p} \mapsto sR\mathbf{p} + \mathbf{t}$ be a similarity transform with rotation $R \in \text{SO}(3)$ (the special orthogonal group, *i.e.*, the group of 3×3 rotation matrices), isotropic scale $s > 0$, and translation $\mathbf{t} \in \mathbb{R}^3$. Translation cancels in the displacement vectors (Eq. (4)) because it is subtracted out when computing differences, while rotation and scaling cancel in the normalised dot product:

$$\frac{(sR\mathbf{u}_k) \cdot (sR\mathbf{v}_k)}{\|sR\mathbf{u}_k\| \|sR\mathbf{v}_k\|} = \frac{s^2 \mathbf{u}_k^\top R^\top R \mathbf{v}_k}{s^2 \|\mathbf{u}_k\| \|\mathbf{v}_k\|} = \frac{\mathbf{u}_k \cdot \mathbf{v}_k}{\|\mathbf{u}_k\| \|\mathbf{v}_k\|}, \quad (7)$$

Hence each angle θ_k is invariant to rotation, translation, and isotropic scaling. This means the angle representation is *intrinsically* portable across datasets captured under different camera configurations—it requires no normalisation preprocessing whatsoever. We verify this theoretical prediction empirically in Sec. 4.6.

Relationship to prior angle features. Joint-angle descriptors are well established in skeleton-based action recognition [7, 22] and classical hand gesture systems [8]. Our contribution is not the angle concept per se but rather its specific instantiation and application: (a) a concrete 20-dimensional formulation defined over the MediaPipe hand topology, (b) a formal $\text{SO}(3)$ -invariance proof accompanied by empirical validation (Sec. 4.6), and (c) a systematic evaluation demonstrating the effectiveness of these invariant features for cross-lingual few-shot sign-language recognition.

3.3. Model Architecture

All models follow a two-stage architecture: an encoder f_ϕ maps a hand-keypoint vector to a 128-dimensional embedding, and a Prototypical Network head [24] classifies queries by nearest-prototype matching in that embedding space. Here, ϕ denotes the trainable parameters of the encoder and $\mathbf{z} = f_\phi(\mathbf{x}) \in \mathbb{R}^{128}$ is the resulting embedding. We evaluate two encoder backbones; both produce embeddings $\mathbf{z} \in \mathbb{R}^{128}$.

MLP encoder. The input vector (63-dimensional for `raw`, 20-dimensional for `angle`, or 83-dimensional for `raw_angle`) passes through two fully connected layers of 256 units each. Each layer applies the sequence

Table 1. Encoder parameter counts by representation. All encoders output 128-D embeddings.

Encoder	Repr	Input Dim	Parameters
MLP	<code>raw</code>	63	116,096
MLP	<code>angle</code>	20	105,088
MLP	<code>raw_angle</code>	83	121,216
Transformer	<code>raw</code>	63	282,240
Transformer	<code>angle</code>	20	284,416
Transformer	<code>raw_angle</code>	83	292,480

`Linear`→`BatchNorm1d`→`ReLU`→`Dropout(0.3)`, followed by a final linear projection to 128 dimensions. The total parameter count ranges from ~ 105 k (`angle`) to ~ 121 k (`raw_angle`); see Tab. 1.

Spatial Transformer encoder. For the `raw` representation, the 21 keypoints are treated as a length-21 token sequence with three-dimensional token embeddings, projected to $d_{\text{model}}=128$ with sinusoidal positional encodings. Two Transformer encoder layers (4 heads, FFN dimension 256, dropout 0.1) apply multi-head self-attention; outputs are mean-pooled across the sequence and projected to 128 dimensions with LayerNorm. For `angle` and `raw_angle` inputs, each angle θ_k spans a multi-keypoint triplet (Eq. (5)), so no natural per-keypoint tokenisation exists. Consequently, the full vector is treated as a single token, and self-attention degenerates to a feedforward path, making the Transformer functionally equivalent to a deeper MLP in this case.

Prototypical Network head. Given an N -way K -shot episode, the prototype for each class n is computed as the mean of its K support embeddings: $\mathbf{c}_n = \frac{1}{K} \sum_{i=1}^K f_\phi(\mathbf{x}_i^{(n)})$. A query sample \mathbf{x}_q with embedding $\mathbf{z}_q = f_\phi(\mathbf{x}_q) \in \mathbb{R}^{128}$ is assigned to the class with the nearest prototype: $\hat{y}_q = \arg \min_n \|\mathbf{z}_q - \mathbf{c}_n\|^2$. Applying a softmax over negative squared distances yields class probabilities. No learnable parameters are introduced beyond those of the encoder.

3.4. Few-Shot Evaluation Protocol

Episode definition. Each episode samples $N=5$ classes from the eligible pool (classes with $\geq K+Q$ test samples), draws K support and $Q=15$ disjoint query examples per class, and classifies queries by nearest prototype [24].

Within-domain evaluation. A randomly initialised encoder is trained and evaluated episodically on each dataset’s own test split, without any pretraining on external data.

Cross-lingual transfer evaluation. The encoder is first pretrained on the source language’s train split using a supervised contrastive loss and then evaluated on each target language under two adaptation modes:

- *Frozen*: all encoder weights are fixed, measuring how well the learned embedding transfers without any adaptation.
- *Target-supervised*: the last linear layer is fine-tuned on the target language’s train split, quantifying the benefit of minimal adaptation.

Reporting. All reported results are averaged over 600 episodes with per-episode random seeds and include 95% confidence intervals.

3.5. Implementation Details

We release the full implementation as a modular, open-source PyTorch codebase.² The key components are summarised below.

Data pipeline (data/). Raw RGB images are processed by MediaPipe Hands v0.10 [29] into per-sample .npy files of shape (21, 3), each storing three-dimensional keypoint coordinates for one hand. A representation layer converts these landmarks on the fly into one of three formats: *raw* (flattened to 63 dimensions), *angle* (20 inter-joint angles from anatomical triplets; Eq. (5)), or *raw_angle* (concatenation of both, 83 dimensions). Deterministic stratified 70/30 train/test splits are stored as JSON files in `splits/` and loaded via `SplitLandmarkDataset`, which validates zero train–test overlap at initialisation.

Episodic sampling (data/episodes.py). A custom `EpisodicSampler` generates N -way K -shot episodes, each seeded by `seed + episode_index` for exact reproducibility. Within each episode, K support and Q query samples per class are drawn without replacement, and a `split_support_query` utility partitions the batch while re-labelling classes to $\{0, \dots, N-1\}$.

Encoders (models/). The MLP encoder (`mlp_encoder.py`) stacks `Linear`→`BatchNorm1d`→`ReLU`→`Dropout(0.3)` blocks followed by a final 128-D projection. The Transformer encoder (`temporal_transformer.py`) projects each of the 21 keypoints from 3-D to $d_{\text{model}}=128$ with sinusoidal positional encodings, applies two self-attention layers (4 heads, FFN 256, dropout 0.1), mean-pools, and projects to 128-D. Both encoders feed into a shared Prototypical Network head (`prototypical.py`). A factory in `models/__init__.py` routes encoder and model construction by name.

Training and losses (train.py, losses/). The training objective combines episode classification loss (negative

²https://github.com/fjkrch/sign_metric_learning

log-likelihood on ProtoNet log-probabilities) with a supervised contrastive (SupCon) loss [16] weighted by 0.5 and using temperature $\tau=0.07$. Optimisation uses AdamW with learning rate 10^{-4} , weight decay 10^{-4} , gradient clipping at 1.0, and a cosine annealing schedule. Early stopping with patience 15 halts training when episode accuracy plateaus.

Cross-lingual adaptation (adapt.py). For cross-lingual transfer, a pretrained checkpoint is loaded, the backbone is optionally frozen, and the last linear layer is fine-tuned on the target language’s train split for up to 20 epochs (learning rate 10^{-4}).

Evaluation and reproducibility (evaluate.py, tools/). Evaluation scripts compute per-episode accuracy with 95% confidence intervals ($1.96 \sigma / \sqrt{n}$) and produce t-SNE visualisations and confusion matrices. Helper scripts in `tools/` automate the full experimental matrix (`run_full_matrix.py`), cross-domain evaluation (`run_cross_domain_expanded.py`), baseline comparisons (`run_baselines.py`), and \LaTeX table export (`export_tables.py`). All experiments are governed by YAML configuration files in `configs/`. Multi-seed robustness checks (seeds 42, 1337, 2024) confirm standard deviations below 1 pp across all datasets.

4. Experiments

We evaluate the proposed geometry-aware representation along four axes: within-domain few-shot performance (Sec. 4.3), cross-lingual transfer from ASL (Sec. 4.4), multi-source transfer (Sec. 4.5), normalisation ablation (Sec. 4.6), and baseline comparison (Sec. 4.7). We conclude with a targeted analysis of the most challenging dataset, Thai fingerspelling (Sec. 4.8).

4.1. Experimental Setup

All experiments run on a consumer CPU (AMD Ryzen 7 7840HS); an NVIDIA GeForce RTX 4060 Laptop GPU is available but not required. Hand-keypoint extraction uses MediaPipe Hands v0.10 [29]; models are implemented in PyTorch 2.10 with the AdamW optimiser; all runs are fully deterministic (seed 42). On this hardware, a single training epoch on ASL (~ 44 k samples) takes approximately 1.5 minutes with the Transformer encoder and under 30 seconds with the MLP; a 600-episode 5-way 5-shot evaluation completes in ~ 7 seconds per dataset.

4.2. Datasets

We evaluate on four fingerspelling datasets drawn from distinct language families (Tab. 2): ASL (American, 29 classes, studio-style RGB) [20], LIBRAS (Brazilian, 21 classes, varied backgrounds) [11], Arabic SL (31 classes, controlled

Table 2. Dataset statistics after MediaPipe extraction and 70/30 splitting (seed 42). Eligible = classes with $\geq K+Q$ test samples at $K=5$, $Q=15$.

Dataset	Classes	Train	Test	Min n_c^{test}	Elig. ($K=5$)
ASL Alphabet [20]	29	44 498	19 093	1	28/29
LIBRAS Alphabet [11]	21	23 993	10 291	447	21/21
Arabic SL [1]	31	4 952	2 141	56	31/31
Thai Finger. [14]	42	1 998	863	12	27/42

capture) [1], and Thai Fingerspelling (42 classes, smallest per-class counts) [14]. In Tab. 2, $\min n_c^{\text{test}}$ denotes the minimum per-class test count, and *Eligible*($K=5$) indicates the number of classes with $\geq K + Q = 20$ test samples. All images are processed through MediaPipe Hands; samples for which no hand is detected are discarded. Splits are deterministic JSON files generated by stratified 70/30 partitioning (seed 42); all reported results use the **test split** exclusively.

4.3. Within-Domain Results: How Discriminative Are Angle Features?

Table 3 reports within-domain few-shot accuracy, where each model is both trained and evaluated on the same dataset. Rows are grouped by dataset; columns compare three input representations across two encoder architectures.

Key findings. On LIBRAS, Arabic, and Thai, the `angle` representation paired with the MLP encoder consistently achieves the highest accuracy. The largest gains over normalised `raw` coordinates appear on Arabic (+25.3 percentage points at 5-shot) and LIBRAS (+12.9 percentage points). On ASL—the largest dataset—the `raw_angle` concatenation slightly outperforms individual representations (95.4%). This is likely because the abundant training data allows the network to exploit complementary coordinate and angle cues, whereas on smaller datasets the additional dimensionality introduces noise that outweighs the benefit. The MLP encoder generally matches or outperforms the Transformer, a finding consistent with Chen *et al.* [6]: simple encoders suffice when the input representation is well designed.

4.4. Cross-Lingual Transfer from ASL: Does Geometric Invariance Reduce Domain Shift?

Table 4 reports few-shot accuracy when the encoder is pre-trained on ASL; the ASL→ASL rows serve as in-domain references (source equals target).

Key findings. With a frozen MLP encoder, `angle` features achieve 95.0% on LIBRAS and 91.3% on Arabic—surpassing `raw` coordinates by 8.5 and 17.1 percentage points, respectively—confirming that geometric invariance substantially reduces cross-dataset domain shift. Target-supervised fine-tuning further improves these results to 96.0% and 92.7%. Notably, the best ASL→Thai result (58.5%) exceeds the within-domain baseline (52.7%; Tab. 3), demonstrating that source-language pretraining benefits even the most challenging target. The consistent target difficulty

ordering—LIBRAS > Arabic > Thai—holds across all representations and adaptation modes.

4.5. Multi-Source Transfer: Which Source Language Works Best?

Table 6 provides a comprehensive view of all source–target transfer pairs: off-diagonal cells report frozen cross-lingual transfer, while diagonal cells show the within-domain baseline (no pretraining; from Tab. 3), enabling direct comparison.

Key findings. Source pretraining frequently outperforms target-only few-shot learning: Arabic→LIBRAS reaches 97.1%, exceeding the within-domain score (94.1%) by 3.0 percentage points; LIBRAS→Arabic (91.7%) exceeds within-domain (89.8%) by 1.9 percentage points; and Arabic→Thai (54.6%) exceeds within-domain (52.7%) by 1.9 percentage points. Table 5 provides the LIBRAS↔Arabic per-representation breakdown. The optimal source language is target-dependent: Arabic is best for LIBRAS (97.1%); LIBRAS for Arabic (91.7%); Arabic for Thai (54.6%); and Thai for ASL (95.1%). The optimal representation also varies with the transfer direction: `angle` dominates under large domain shift (e.g., ASL→Arabic), `raw` when the target features standardised capture conditions (ASL), and `raw_angle` for LIBRAS↔Arabic (Tab. 5). The LIBRAS↔Arabic asymmetry may partly reflect differences in dataset scale: LIBRAS provides a richer pretraining signal (23 993 vs. 4 952 train samples; Tab. 2) with more varied backgrounds. Across both non-ASL transfer directions, `raw_angle` is the best or tied-best representation (Tab. 5), suggesting that combining positional and angular cues compensates for moderate domain shift when neither component alone suffices.

4.6. Normalisation Ablation: Are Angles Truly Invariant?

Table 7 provides empirical verification of the theoretical invariance claim: removing both wrist-centring and scale normalisation degrades `raw` coordinates by 4.8–5.4 percentage points, whereas `angle` features remain virtually unchanged ($|\Delta| \leq 0.3$ percentage points), confirming the prediction of Eq. (7). A more granular decomposition on Arabic (Tab. 8) reveals the contribution of each processing stage:

The geometry-aware `angle` representation provides the single largest improvement—a mean absolute gain of 25.3 percentage points at 5-shot over normalised `raw` coordinates—demonstrating that the benefit extends well beyond preprocessing to the construction of a more discriminative feature space.

Table 3. Within-domain few-shot accuracy (%) on the **test split**. 5-way K -shot, $Q=15$, ProtoNet (Euclidean), 600 episodes, seed 42. Bold = best accuracy per dataset across all representations and encoders.

Dataset	Repr.	MLP Encoder			Transformer Encoder		
		1-shot	3-shot	5-shot	1-shot	3-shot	5-shot
ASL	raw	88.7±0.7	93.8±0.5	94.9±0.4	74.2±1.0	80.3±0.9	82.1±0.9
	angle	81.5±0.9	86.8±0.7	88.4±0.6	80.8±0.9	86.2±0.7	87.7±0.7
	raw_angle	90.4±0.7	94.5±0.5	95.4±0.4	90.8±0.7	94.7±0.4	95.4±0.4
LIBRAS	raw	69.7±1.0	78.9±0.8	81.2±0.8	61.1±0.9	65.9±0.9	67.9±0.9
	angle	89.2±0.7	92.9±0.5	94.1±0.5	86.9±0.8	91.1±0.6	92.5±0.5
	raw_angle	71.6±1.0	82.2±0.8	84.6±0.8	72.8±1.0	82.3±0.8	84.7±0.7
Arabic	raw	51.3±0.9	60.6±0.8	64.5±0.8	43.1±0.9	47.1±1.0	49.0±0.9
	angle	81.1±0.9	88.2±0.6	89.8±0.6	78.3±0.9	85.7±0.7	87.8±0.6
	raw_angle	55.5±1.0	66.6±0.9	71.0±0.9	55.6±1.0	63.2±0.9	67.3±0.9
Thai	raw	40.3±0.7	47.0±0.7	48.8±0.8	33.3±0.7	35.7±0.6	36.0±0.6
	angle	46.2±0.8	51.2±0.8	52.7±0.8	44.6±0.8	50.6±0.8	51.8±0.8
	raw_angle	43.4±0.8	50.2±0.8	51.9±0.8	42.3±0.7	47.1±0.7	48.7±0.8

Table 4. Effect of ASL pretraining on few-shot accuracy (%): encoder pretrained on ASL (SupCon), evaluated on each target’s **test split**. 5-way 5-shot, $Q=15$, 600 episodes, seed 42. Bold = best accuracy within each (target, mode) pair across all representations and encoders. ASL→ASL rows are in-domain references (source=target), not cross-lingual transfer. †

Target	Mode	MLP Encoder			Transformer Encoder		
		raw	angle	raw_angle	raw	angle	raw_angle
ASL	Frozen	97.0±0.4	91.7±0.5	97.1±0.4	92.7±0.6	87.5±0.7	97.1±0.3
	Target-sup.	97.0±0.4	91.7±0.5	97.1±0.4	92.7±0.6	87.5±0.7	97.1±0.3
LIBRAS	Frozen	86.5±0.8	95.0±0.4	87.8±0.7	81.3±0.8	93.2±0.5	88.3±0.7
	Target-sup.	94.2±0.5	96.0±0.4	95.2±0.5	81.4±0.8	93.2±0.5	88.4±0.7
Arabic	Frozen	74.2±0.8	91.3±0.5	76.6±0.9	66.1±0.9	87.4±0.7	75.9±0.9
	Target-sup.	89.4±0.6	92.7±0.5	92.9±0.5	66.2±0.9	87.4±0.7	76.2±0.8
Thai	Frozen	52.5±0.9	53.2±0.8	50.6±0.8	48.7±0.8	48.8±0.8	53.8±0.8
	Target-sup.	58.5±0.9	57.4±0.8	57.3±0.8	48.8±0.8	48.8±0.8	53.9±0.8

† ASL→ASL (source=target) is an in-domain reference, not cross-lingual transfer.

Table 5. Multi-source transfer: LIBRAS↔Arabic per-representation breakdown (MLP, 5-way 5-shot, $Q=15$, 600 episodes, seed 42). Bold = best representation within each (direction, mode) pair.

Direction	Repr	Frozen	Target-sup.
LIBRAS→Arabic	raw	89.8±0.6	91.8±0.6
	angle	91.2±0.6	92.2±0.5
	raw_angle	91.7±0.6	93.8±0.5
Arabic→LIBRAS	raw	95.9±0.5	96.5±0.4
	angle	94.9±0.5	95.9±0.4
	raw_angle	97.1±0.4	97.4±0.4

4.7. Baselines and Robustness: How Much Does the Encoder Help?

To disentangle the encoder’s contribution from that of the representation itself, Tab. 9 compares three 5-way 5-shot classification methods: (i) *input-space* nearest prototype

Table 6. Best accuracy (%) by source language (MLP, 5-way 5-shot, $Q=15$, 600 episodes, seed 42). Off-diagonal: frozen-encoder transfer; each cell reports the highest-scoring representation (parenthesized: r=raw, a=angle, ra=raw_angle). Diagonal†: within-domain baseline (no pretraining; from Tab. 3). Bold = best cross-lingual source for each target row.

Target	ASL	LIBRAS	Arabic	Thai
ASL	95.4±0.4† (ra)	93.7±0.5 (r)	94.1±0.4 (r)	95.1±0.4 (ra)
LIBRAS	95.0±0.4 (a)	94.1±0.5† (a)	97.1±0.4 (ra)	94.6±0.5 (a)
Arabic	91.3±0.5 (a)	91.7±0.6 (ra)	89.8±0.6† (a)	90.2±0.5 (a)
Thai	53.2±0.8 (a)	52.2±0.8 (ra)	54.6±0.9 (r)	52.7±0.8† (a)

† Within-domain (no pretraining); all other cells use frozen cross-lingual transfer.

(no encoder; Euclidean distance computed directly in the raw feature space), (ii) *episode-linear* (per-episode logistic regression fitted on MLP support embeddings), and (iii) our ProtoNet with an MLP encoder.

Key findings. The input-space baseline is competitive with ProtoNet on several datasets (e.g., ASL/raw: 95.1%

Table 7. Effect of removing wrist-centring and scale normalisation. 5-way 5-shot, $Q=15$, MLP encoder, 600 episodes, seed 42. “No norm” = MediaPipe raw output.

Dataset	Repr	No Norm	Normalised	Diff. (p.p.)
LIBRAS	raw	76.4	81.2	4.8
LIBRAS	angle	94.4	94.1	-0.3 [†]
Arabic	raw	59.1	64.5	5.4
Arabic	angle	90.1	89.8	-0.3 [†]

[†]Within noise band; confirms theoretical invariance (Eq. (7)).

Table 8. Cumulative normalisation ablation on Arabic (MLP / raw). 5-way K -shot, $Q=15$, 600 episodes, seed 42.

Setting	1-shot	3-shot	5-shot
No normalisation	41.8	56.3	59.1
+ Wrist-centring & scale	51.3	60.6	64.5
+ Geometry-aware (angle)	81.1	88.2	89.8

Table 9. Baseline comparison (5-way 5-shot, $Q=15$, 600 episodes, seed 42, MLP encoder where applicable).

Dataset	Repr	Input-Sp.	Ep.-Linear	ProtoNet
ASL	raw	95.1±0.4	91.9±0.5	94.9±0.4
ASL	angle	89.4±0.6	85.7±0.7	88.4±0.6
LIBRAS	raw	81.0±0.8	80.2±0.8	81.2±0.8
LIBRAS	angle	94.2±0.5	93.1±0.5	94.1±0.5
Arabic	raw	65.0±0.9	63.7±0.9	64.5±0.8
Arabic	angle	90.5±0.6	88.2±0.6	89.8±0.6
Thai	raw	47.6±0.8	50.9±0.8	48.8±0.8
Thai	angle	52.8±0.8	51.9±0.8	52.7±0.8

vs. 94.9%), confirming that hand-keypoint features are inherently discriminative. A full-data linear classifier attains 99.7% on LIBRAS and 93.8% on ASL; the gap to 5-shot ProtoNet (5.6 pp on LIBRAS) quantifies the cost of learning from only five examples. On Thai, ProtoNet slightly exceeds the full-data classifier (52.7% vs. 51.7%), likely because the limited number of training samples per class (~ 48) constrains the linear model. Multi-seed evaluation (seeds 42, 1337, 2024) yields standard deviations below 1 pp on all datasets, confirming the robustness of these results.

4.8. Analysis: Why Is Thai Fingerspelling Difficult?

Thai yields the lowest accuracy among all four datasets. Three factors contribute to this difficulty: the high class cardinality (42 classes), the small dataset size (~ 2860 samples after filtering), and the existence of consonant groups with similar hand shapes. Despite these challenges, `angle` features outperform `raw` by 3.9 pp at 5-shot (Tab. 3), and ASL \rightarrow Thai transfer (53.2%; Tab. 6) slightly exceeds the within-domain baseline (52.7%).

Figure 3 shows per-class accuracy spanning 26–94%; confusions concentrate on morphologically similar consonant pairs (e.g., classes 13 \rightarrow 14, 28 \rightarrow 4), suggesting that

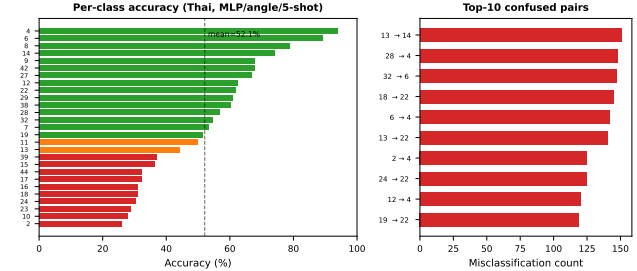


Figure 3. Error analysis on Thai (MLP / angle / 5-way 5-shot, 600 episodes). **Left:** Per-class accuracy (26–94%). **Right:** Top 10 confused pairs.

finer-grained features—such as bone-length ratios or contact information—may be needed to disambiguate these cases.

5. Discussion

Why invariant features help few-shot transfer. In Prototypical Networks, each class centroid is a sample mean over only K support examples. When the input representation carries extrinsic variance—due to camera viewpoint, hand scale, or global position—the centroid estimate is corrupted by factors unrelated to hand shape, and classification degrades. The $SO(3)$ -invariant angle representation (Eq. (7)) eliminates these nuisance factors at the representation level, compressing hand-pose information into a 20-dimensional space where class prototypes are geometrically tighter. This is particularly critical in the few-shot regime ($K=5$), where there is insufficient data to learn invariance from examples alone (Tab. 8). The empirical consequence is that pretraining on any source language can outperform target-only few-shot training—for example, Arabic \rightarrow LIBRAS with a frozen encoder exceeds within-domain accuracy by 3.0 pp (Tab. 6)—indicating that the invariant embedding captures portable geometric structure that transfers across sign languages.

When do coordinate features still help? On ASL, the largest and most uniformly captured dataset, the `raw_angle` concatenation achieves the best results (Tabs. 3 and 4). This suggests that when domain shift is small and data are abundant, absolute positional cues provide complementary discriminative information that angles alone discard. For LIBRAS \leftrightarrow Arabic transfer, `raw_angle` likewise outperforms `angle` alone (Tab. 5), indicating that moderate domain shift does not fully negate the value of coordinate features.

Limitations. Several limitations should be noted. First, our evaluation covers *static fingerspelling only*; dynamic signs and continuous signing involve temporal trajectories that require sequential modelling. Second, we use *single-hand keypoints*: two-handed signs and signs involving body or facial cues are outside the current scope. Third, the angle

representation *discards absolute bone-length information*, which could be discriminative for signs that differ primarily in finger extension magnitude or hand size. Finally, although we evaluate four typologically diverse languages, broader coverage—especially of non-fingerspelling sign lexicons—is needed to assess generality.

6. Conclusion

Scaling sign-language recognition to the majority of the world’s 300+ sign languages demands methods for cross-lingual few-shot transfer from data-rich source languages. We introduced a 20-dimensional SO(3)-invariant joint-angle descriptor that removes a dominant source of cross-dataset domain shift and stabilises Prototypical Network classification across languages. Evaluated under a unified, deterministic episodic protocol across four typologically diverse fingerspelling alphabets, angle-based features consistently improve over normalised-coordinate baselines, with the largest gains observed under substantial domain shift. The `raw_angle` concatenation frequently emerges as the strongest cross-lingual representation, although the optimal choice remains direction-dependent. These results demonstrate that formally invariant hand-geometry descriptors can serve as a portable and effective foundation for few-shot sign-language recognition in low-resource settings.

References

- [1] Muhammad Al-Brham. RGB Arabic alphabets sign language dataset, 2023. Kaggle, <https://www.kaggle.com/datasets/muhammadalbrham/rgb-arabic-alphabets-sign-language-dataset>.
- [2] Ahmed A. Alani and Georgina Cosma. ArSL-CNN: A convolutional neural network for arabic sign language gesture recognition. In *Proceedings of the International Joint Conference on Neural Networks (IJCNN)*, pages 1–8, 2021.
- [3] Yunus Can Bilge, Nazli Ikizler-Cinbis, and Ramazan Gokberk Cinbis. Towards zero-shot sign language recognition. *Pattern Recognition*, 150:110351, 2024.
- [4] Matyáš Boháček. Pose-based few-shot sign language recognition. *arXiv preprint arXiv:2301.03769*, 2023.
- [5] Necati Cihan Camgöz, Oscar Koller, Simon Hadfield, and Richard Bowden. Sign language transformers: Joint end-to-end sign language recognition and translation. In *Proceedings of the IEEE/CVF Conference on Computer Vision and Pattern Recognition (CVPR)*, pages 10023–10033, 2020.
- [6] Wei-Yu Chen, Yen-Cheng Liu, Zsolt Kira, Yu-Chiang Frank Wang, and Jia-Bin Huang. A closer look at few-shot classification. In *Proceedings of the International Conference on Learning Representations (ICLR)*, 2019.
- [7] Yuxin Chen, Ziqi Zhang, Chunfeng Yuan, Bing Li, Ying Deng, and Weiming Hu. Channel-wise topology refinement graph convolution for skeleton-based action recognition. In *Proceedings of the IEEE/CVF International Conference on Computer Vision (ICCV)*, pages 13026–13035, 2021.
- [8] Ming Jin Cheok, Zaid Omar, and Mohamed Hasan Jaward. A review of hand gesture and sign language recognition techniques. *International Journal of Machine Learning and Cybernetics*, 10(1):131–153, 2019.
- [9] Alexis Conneau, Kartikay Khandelwal, Naman Goyal, Vishrav Chaudhary, Guillaume Wenzek, Francisco Guzmán, Edouard Grave, Myle Ott, Luke Zettlemoyer, and Veselin Stoyanov. Unsupervised cross-lingual representation learning at scale. In *Proceedings of the Annual Meeting of the Association for Computational Linguistics (ACL)*, pages 8440–8451, 2020.
- [10] Cláudio Carvalho de Amorim, David Macêdo, and Cleber Zanchettin. Sign language recognition using skeleton data with MediaPipe. In *Proceedings of the International Joint Conference on Neural Networks (IJCNN)*, pages 1–8, 2023.
- [11] Willian Soares de Oliveira. LIBRAS: Brazilian Sign Language alphabet dataset, 2022. Kaggle, <https://www.kaggle.com/datasets/williansoliveira/libras>.
- [12] Ethnologue. Sign languages of the world, 2024. <https://www.ethnologue.com>.
- [13] Chelsea Finn, Pieter Abbeel, and Sergey Levine. Model-agnostic meta-learning for fast adaptation of deep networks. In *Proceedings of the International Conference on Machine Learning (ICML)*, pages 1126–1135, 2017.
- [14] Nicki Hartmann. Thai letter sign language dataset, 2023. Kaggle, <https://www.kaggle.com/datasets/nickihartmann/thai-letter-sign-language>.
- [15] Songyao Jiang, Bin Sun, Ling Wang, Yue Bai, Kunpeng Li, and Yun Fu. Skeleton aware multi-modal sign language recognition. In *Proceedings of the IEEE/CVF Conference on Computer Vision and Pattern Recognition Workshops (CVPRW)*, pages 3413–3423, 2021.
- [16] Prannay Khosla, Piotr Teterwak, Chen Wang, Aaron Sarna, Yonglong Tian, Phillip Isola, Aaron Maschinot, Ce Liu, and Dilip Krishnan. Supervised contrastive learning. In *Advances in Neural Information Processing Systems (NeurIPS)*, pages 18661–18673, 2020.
- [17] Dongxu Li, Cristian Rodriguez-Opazo, Xin Yu, and Hongdong Li. Word-level deep sign language recognition from video: A new large-scale dataset and methods comparison. In *Proceedings of the IEEE/CVF Winter Conference on Applications of Computer Vision (WACV)*, pages 1459–1469, 2020.
- [18] Xian Li, Changan Wang, Yun Tang, Chau Tran, Yuqing Tang, Dieysa Juan, Alexei Baevski, and Michael Auli. Massively multilingual ASR: 50 languages, 1 model, 1 billion parameters. In *Proceedings of Interspeech*, pages 4751–4755, 2022.
- [19] Akash Mavi. A real-time applicable 3d hand gesture recognition system using deep learning with ASL dataset. *International Journal of Intelligent Systems and Applications in Engineering*, 8(4):204–212, 2020.
- [20] Akash Nagaraj. ASL alphabet: Image dataset for alphabets in American Sign Language, 2018. Kaggle, <https://www.kaggle.com/datasets/grassknotted/asl-alphabet>.
- [21] Kaushik Kumar Podder, Muhammad E. H. Chowdhury, Anas M. Tahir, Zaid Bin Mahbub, Amith Khandakar,

- Md. Shafayet Hossain, and Tawil O. Abbas. Bangla sign language (BdSL) alphabets & numerals classification using a deep learning model. *Sensors*, 22(2):574, 2022.
- [22] Lei Shi, Yifan Zhang, Jian Cheng, and Hanqing Lu. Two-stream adaptive graph convolutional networks for skeleton-based action recognition. In *Proceedings of the IEEE/CVF Conference on Computer Vision and Pattern Recognition (CVPR)*, pages 12026–12035, 2019.
- [23] Jungpil Shin, Md. Al Mehedi Musa, and Md. Al Mehedi Hasan. Korean sign language recognition using MediaPipe and deep learning. In *International Conference on Big Data and Smart Computing (BigComp)*, pages 365–368, 2023.
- [24] Jake Snell, Kevin Swersky, and Richard S. Zemel. Prototypical networks for few-shot learning. In *Advances in Neural Information Processing Systems (NeurIPS)*, pages 4077–4087, 2017.
- [25] Flood Sung, Yongxin Yang, Li Zhang, Tao Xiang, Philip H. S. Torr, and Timothy M. Hospedales. Learning to compare: Relation network for few-shot learning. In *Proceedings of the IEEE/CVF Conference on Computer Vision and Pattern Recognition (CVPR)*, pages 1199–1208, 2018.
- [26] Federico Tavella, Viktor Schlegel, Marta Romeo, Martin Kolaček, and Baptiste Caramiaux. Few-shot sign language recognition with transfer learning. In *Proceedings of the LREC Workshop on Resources and Technologies for Indigenous, Endangered and Lesser-resourced Languages*, pages 94–100, 2022.
- [27] Oriol Vinyals, Charles Blundell, Timothy Lillicrap, Koray Kavukcuoglu, and Daan Wierstra. Matching networks for one shot learning. In *Advances in Neural Information Processing Systems (NeurIPS)*, pages 3630–3638, 2016.
- [28] World Health Organization. Deafness and hearing loss, 2024. Fact sheet, <https://www.who.int/news-room/fact-sheets/detail/deafness-and-hearing-loss>.
- [29] Fan Zhang, Valentin Bazarevsky, Andrey Vakunov, Andrei Tkachenka, George Sung, Chuo-Ling Chang, and Matthias Grundmann. MediaPipe Hands: On-device real-time hand tracking. *arXiv preprint arXiv:2006.10214*, 2020.